J Fluoresc (2014) 24:983–989
DOI 10.1007/s10895-014-1388-x

SHORT COMMUNICATION

Automated Enumeration and Viability Measurement of Canine Stromal Vascular Fraction Cells Using Fluorescence-Based Image Cytometry Method

Leo Li-Ying Chan · Donald A. Cohen · Dmitry Kuksin · Benjamin D. Paradis · Jean Qiu

Received: 31 December 2013 / Accepted: 7 April 2014 / Published online: 17 April 2014

Abstract In recent years, the lipoaspirate collected from adipose tissue has been seen as a valuable source of adipose-derived mesenchymal stem cells for autologous cellular therapy [1–3]. For multiple applications, adipose-derived mesenchymal stem cells are isolated from the stromal vascular fraction (SVF) of adipose tissue. Because the fresh stromal vascular fraction typically contains a heterogeneous mixture of cells [4, 5], determining cell concentration and viability is a crucial step in preparing fraction samples for downstream processing. Due to a large amount of cellular debris contained in the SVF sample, as well as counting irregularities standard manual counting can lead to inconsistent results. Advancements in imaging and optics technologies have significantly improved the image-based cytometric analysis method. In this work, we validated the use of fluorescence-based image cytometry for SVF concentration and viability measurement, by comparing to standard flow cytometry and manual hemocytometer. The concentration and viability of freshly collected canine SVF samples are analyzed, and the results highly correlated between all three methods, which validated the image cytometry method for canine SVF analysis, and potentially for SVF from other species.

Keywords Stromal Vascular Fraction (SVF) · Adipose-derived mesenchymal stem cell · Concentration · Viability · Acridine orange · Propidium iodide · Image cytometry · Cellometer

L. L.-Y. Chan (✉) · D. Kuksin · B. D. Paradis · J. Qiu
Department of Technology R&D, Nexcelom Bioscience LLC, 360 Merrimack St. Building 9, Lawrence, MA 01843, USA
e-mail: lchan@nexcelom.com

D. A. Cohen
Department of Microbiology, Immunology, and Molecular Genetics, College of Medicine, University of Kentucky, Lexington, KY 40508, USA

Introduction

The use of mesenchymal stem cells (MSCs) in regenerative medicine holds great promise for repair of tissues damaged by a number of acute conditions, such as injuries to tendons, ligaments, bone or cartilage and for chronic conditions, such as osteoarthritis. MSCs have been isolated from a number of different tissue sources within the body, such as bone marrow, blood, adipose tissue, muscle and cartilage [6–9]. While many basic and clinical studies were performed initially using bone marrow-derived MSCs, the fact that MSCs are present in adipose tissues at 100–1,000 times greater concentrations than in bone marrow has led to greater interest in adipose-derived MSCs for regenerative stem cell therapy [10–12]. MSCs obtained from the stromal vascular fraction (SVF) of adipose tissue, possess multi-lineage differentiation capacity, which allows them to develop into a variety of cell types, including chondrocytes, osteoblasts, myocytes cells and others [13–23]. SVF of adipose tissue contains a heterogeneous mixture of cells, including not only MSCs, but also variable numbers of endothelial cells, smooth muscle cells, fibroblasts, preadipocytes and immune cells [24, 25]. SVF preparations have been used either as a source of fresh MSCs (albeit, in low cell concentrations) or in culture as a means to expand MSCs in vitro. Regardless of their final usage, accurate determination of cell concentrations and viability in freshly isolated adipose SVF is critical in order to achieve the expected basic or clinical research outcomes.

Cell concentration and viability of SVF preparations are usually determined by standard hemocytometer methods. Hemocytometer counting can be subjected to considerable error since the person counting cells must make judgments between actual cells versus "debris", a task made more difficult by the range of particle sizes present in SVF preparations. The presence of erythrocytes, platelets and cellular debris in SVF preparations creates a substantial amount of "noise" which must be

distinguished from actual cells. Failure to appropriately account for this noise can lead to inaccurate cell counts. Recently, there has been an increase in the adaptation of automated image-based cytometers due to increased availability of this technology in the field. Technological advancements in imaging detectors, low-cost light sources, optical lenses, and imaging analysis software allowed the development of more affordable image-based cytometry systems [26]. Image-based cytometers via bright-field analysis have been utilized to perform cell concentration and viability (trypan blue exclusion) measurements in order to replace current manual counting methods [27, 28]. With the addition of fluorescence capabilities, a variety of dual-fluorescence viability stain combinations such as acridine orange (AO)/propidium iodide (PI), Hoechst 33342 (HO)/PI, CFDA/PI, and Calcein AM/PI can be used to analyze primary cells with high erythrocytes or red blood cell (RBC) contamination, and cell samples containing high debris content [28–30]. In addition, image-based cytometric analysis allows visual confirmation of the counted live and dead cells, which can validate the analyzed fluorescent data.

Previously, Cellometer image cytometry has been shown to perform both bright-field and fluorescence-based cell concentration and viability measurements [26]. The image-based method utilizes a dual-staining protocol of two nuclear fluorescent dyes, AO and PI, to specifically stain membrane-intact live cells and membrane-compromised dead cells. This method allows accurate identification of nucleated cells in a complex sample containing RBCs, platelets, and cellular debris to measure concentration and viability. In this work, we validate the automated image cytometry method for SVF analysis. First, the imaging parameters were optimized by measuring five adipose SVF samples. Next, the concentration and viability of three freshly prepared SVF cell samples were measured and compared using hemocytometer, flow cytometer, and image cytometer methods using trypan blue (TB) and HO/PI. In addition, AO/PI was used to measure concentration and viability for the image cytometry method for comparison to HO/PI. The results show comparable concentration measurements amongst the detection methods used, and show that automated image-based cytometry can be used to efficiently generate accurate SVF measurements.

Materials and Methods

SVF Sample Preparation

Stromal vascular fractions (SVF) were graciously provided by MediVet-America, Inc. from freshly collected canine adipose tissue of individual subjects, using their proprietary methods for processing of adipose tissue. The SVF samples were transported on ice to the University of Kentucky for analysis within 2 h of tissue processing. Within 1 h of sample receipt, each sample was initially stained with trypan blue and counted manually on a hemocytometer using standard procedures. The same samples were then analyzed by flow cytometry and image cytometry approaches. Initially, concentrations of five independent samples (A–E) were measured and compared using flow cytometry, image cytometry, and hemocytometer, in order to understand the characteristics of these SVF samples. Next, viability and concentrations were compared for two more individual samples (1–2).

Hemocytometer Protocol

Fresh SVF samples were diluted 1:100 in PBS and subsequently 1:10 in trypan blue to yield a final concentration of 1:1,000. The average of two full squares was used to calculate the % viable and dead cells per ml of the SVF sample. The method was performed for the first 5 samples and then the 2 individual samples. Manual counting by Neubauer hemocytometer was performed on 4 replicate dilutions for each sample and the mean +/− standard deviation was determined.

Cellometer Image Cytometry Protocol

Fresh SVF samples were diluted 1:100 in PBS. Diluted SVF was stained 1:1 with AO/PI dual-staining solution (Nexcelom Bioscience) and HO/PI solution (2× stock solution). The HO/PI staining solution (75 μl) was mixed with cell sample (75 μl) and incubated in the dark for 45 min in a 37 °C water bath before image cytometric analysis. Twenty microliters of sample was mixed uniformly with 20 μl of AO/PI and immediately pipetted (20 μl) into a Nexcelom counting chamber. The counting chamber was then inserted into the image cytometer for automated image analysis to measure concentration and viability of the SVF samples. Bright-field and fluorescent images were captured at four different locations, where the AO/PI and HO/PI fluorescent images were counted to determine the live and dead cell count in the sample. The cell size parameters were setup to count only nucleated cells and not the cell debris (4–50 μm). Next, fluorescence thresholds were setup to count only fluorescent positive cells stained with AO (threshold: 15), HO (threshold: 10), and PI (threshold: 35). The AO/PI method was performed for the five optimization samples to measure concentrations. Both AO/PI and HO/PI were performed to compare multiple concentration and viability methods using the final two individual samples. The concentration and viability measurements were performed in quadruplicates.

The Cellometer software utilized the Fluorescence 1 and Fluorescence 2 imaging mode to generate cell counts for live cells (AO- and HO-positive) and dead cells (PI-positive). The cell counts were then used to automatically generate concentration and viability data with a dilution factor of 2. Cellometer Vision image cytometer was used for SVF measurement using fluorescence optics modules (FOMs) VB-535-402 (EX:

470 nm, EM: 535 nm), VB-450-302 (EX: 375 nm, EM: 450 nm), and VB-660-502 (EX: 540 nm, EM: 660 nm) for AO, HO, and PI detection, respectively. The system utilized a 5× magnification for image collection.

Flow Cytometry Protocol

Fresh SVF samples were diluted 1:100 in PBS. Diluted SVF (75 μl) was mixed with 75 μl of HO/PI solution (2× stock) and the mixture was incubated for 45 min in a 37 °C water bath. CytoCount beads (Dako) (150 μl) were added the mixture was analyzed on a Synergy Cell Sorter (iCyt/Sony) by counting 10,000 beads. The ratio of beads to Hoechst-positive cells (gated on canine PBMCs for cell size) was used to determine the % of viable and dead (PI positive) cells per ml of the SVF sample. The Synergy Cell Sorter utilized an excitation wavelength of 355 and 488 nm for excitation of HO and PI, respectively. The method was performed for the first 5 samples and the final 2 individual samples.

Gating Protocol for Flow Cytometry Counting

An initial gate was set on paraformaldehyde-fixed canine peripheral blood mononuclear cells (PBMCs) to exclude events that were smaller than PBMCs (cell size gate). The cell size gate was then transferred onto the SVF sample to identify PBMC sized cells. A second gate was set on Hoechst positive events to identify nucleated cells in the SVF. A third gate was set on PI negative cells to determine the percent viable cells. Finally, a fourth gate was set on the counting beads so a count of 10,000 beads could be established. The gating scheme is shown in Fig. 1.

Results and Discussion

Bright-Field and Fluorescent Image Analysis

Figure 2 shows the bright-field and fluorescent images of SVF stained with AO/PI or HO/PI. There are numerous cellular debris and non-nucleated particles that can be observed in the bright-field images, which showed weak to no fluorescence signals. It is obvious that if one is to manually count the SVF samples without proper training on counting specification, human-error can be introduced. The fluorescent images showed bright and dim populations, which are used to gate the live, dead, and non-nucleated cells.

Initial Concentration Optimization

Concentrations of the initial five independent SVF samples were measured using hemocytometer, image cytometry, and flow cytometry methods. Figure 3 shows concentration measurement comparison using each method. Although the image analysis counting parameters were not optimized in this experiment, the comparisons showed similar results for Samples A–D, where a deviation of ±10 % occurred. For Sample E, there is a large discrepancy between the manual hemocytometer counting versus the automated image and flow cytometry method, which could be due to the difficulty in identifying cell particles for a highly concentrated sample. Overall, this experiment allowed optimization of image cytometry parameters to measure specific cell particles stained with AO/PI that was comparable to flow cytometry.

Concentration Measurement Comparison

Concentrations of the final 2 SVF samples were measured using hemocytometer, image cytometry, and flow cytometry methods. For the image cytometry method, both AO/PI and HO/PI were used to stain the SVF samples, while flow cytometry method only used HO/PI. The concentration results are plotted in a bar graph shown in Fig. 4a. By using optimized parameters from the initial experiment, concentrations measured for the 2 samples were comparable between the 3 detection methods at a deviation of less than 10 %. Specifically, concentrations measured for sample 2 showed a deviation of less than 3 %. A 2-Sample *T* Test was conducted for comparing the detection methods for both samples. The *p*-values for AO/PI compared to HO/PI using image and flow cytometry, and manual hemocytometer are all greater than 0.05, which means that the results are statistically the same. In sample 1, the hemocytometer measurement showed ~10 % difference compared to image and flow cytometry method, which increased the overall deviation. The increase in cell count could potentially be due to over counting of cellular debris and RBCs. Since both image and flow cytometry method required fluorescent nucleic acid dyes, the results are more comparable, whereas hemocytometer method seemed to generate higher variation. If a comparison is generated between only image and flow cytometry, the deviations for sample 1 and 2 become less than 5 % and 2 %, respectively.

Viability Measurement Comparison

Viabilities of the SVF samples were measured using hemocytometer, image, and flow cytometry through the use of TB, AO/PI, and HO/PI. The comparison of viability results is shown in Fig. 4b. A 2-Sample *T* Test was conducted for comparing the detection methods for both samples. Viability results from the image cytometer using AO/PI and HO/PI were highly comparable to the flow cytometer data. The *p*-values for AO/PI compared to HO/PI using image and flow cytometry are greater than 0.05, which means that the results are statistically the same. However, the TB manual counting method showed a significant reduction in the viability results

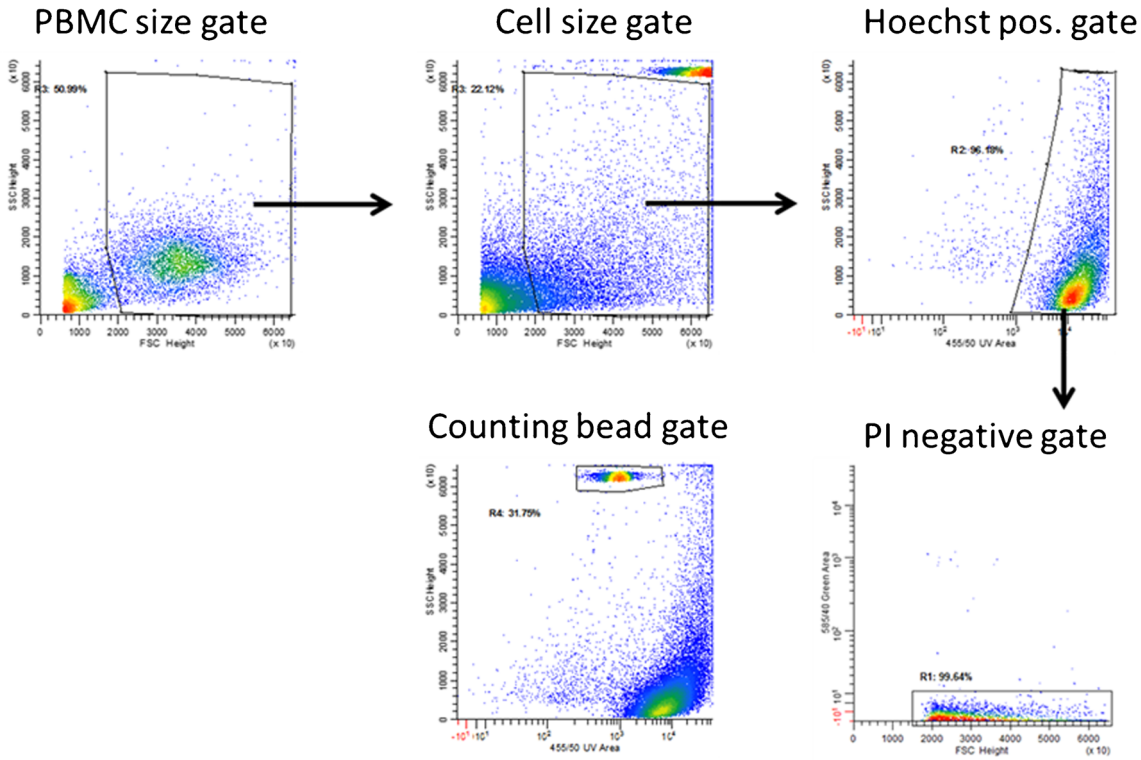

Fig. 1 Flow cytometric analysis gating scheme. Initially, canine PBMCs were used to set the initial cell size gating. Next, the cell size gate was transferred onto each SVF sample. A Hoechst fluorescence gate was set to identify nucleated SVF cells and a propidium iodide fluorescence gate was set to determine the percent viable cells. Finally, a gate was set on the counting beads to determine the concentration of the SVF sample

at ~87 and 83 %, where the *p*-value for AO/PI compared to manual hemocytometer is less than 0.05, which means that the results are not statistically the same. This reduction may have been due to toxic effects of TB on the viability of cells, which has been shown previously, where exposure to TB can increase the rate of cell death after 5 min of staining [31].

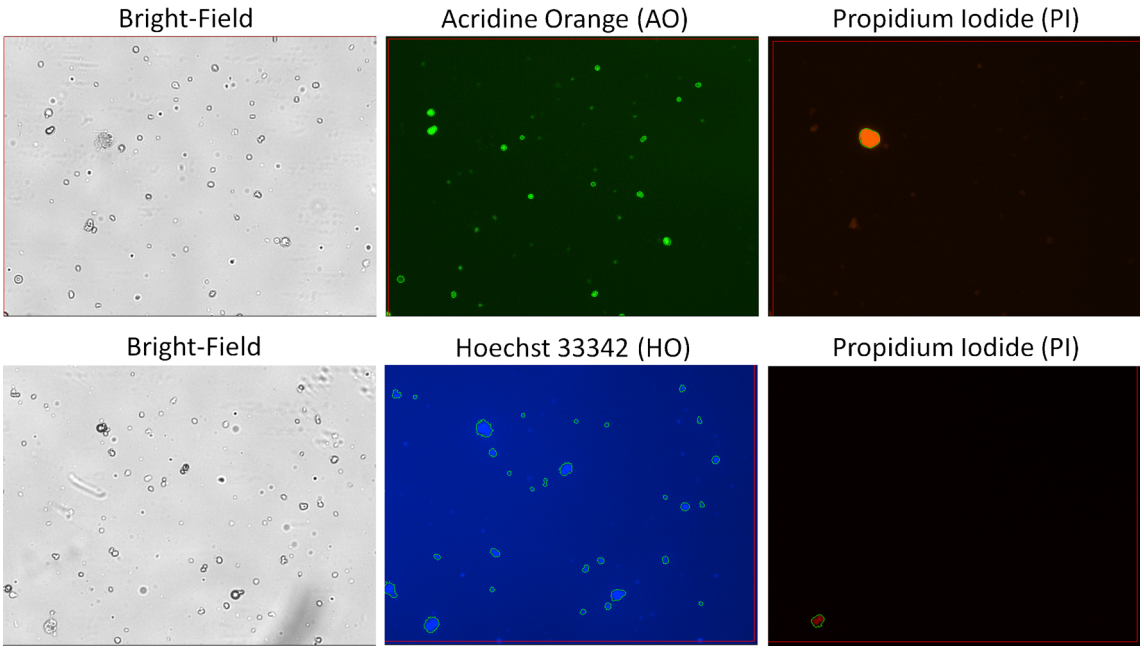

Fig. 2 Bright-field and fluorescent images of SVF samples stained with AO/PI and HO/PI with pseudo color of *green* (AO), *orange* (PI), and *blue* (HO). The bright-field images showed numerous fluorescent and non-fluorescent particles, indicating nucleated cells and cellular debris, respectively

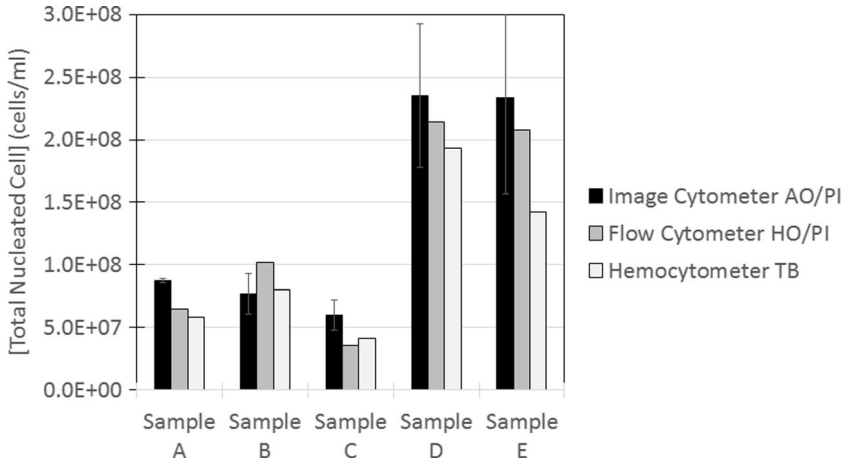

Fig. 3 Concentration comparison results of 5 SVF samples between hemocytometer, image and flow cytometry method. The experiment was conducted to optimize imaging parameters for the image cytometry method, which showed comparable concentration analysis for Sample A–D between all three methods. The deviations were approximately ±10 %. As for Sample E, the image and flow cytometry method showed good correlation. In contrast, the hemocytometer result was approximately 30 % lower, which may indicate the difficulty of manual counting highly concentrated samples (Similar trend shown in Sample D, where hemocytometer result was lower)

Manual counting using a hemocytometer often requires longer time, which is dependent of the concentration and the complexity of the sample. With the complexity of SVF samples containing cellular debris and RBCs, the counting time may have affected the viability using TB. Statistically, manual counting methods may yield approximately 10 % or higher deviation depending on the number of cells counted (typically 100 cells), whereas image or flow cytometers can rapidly

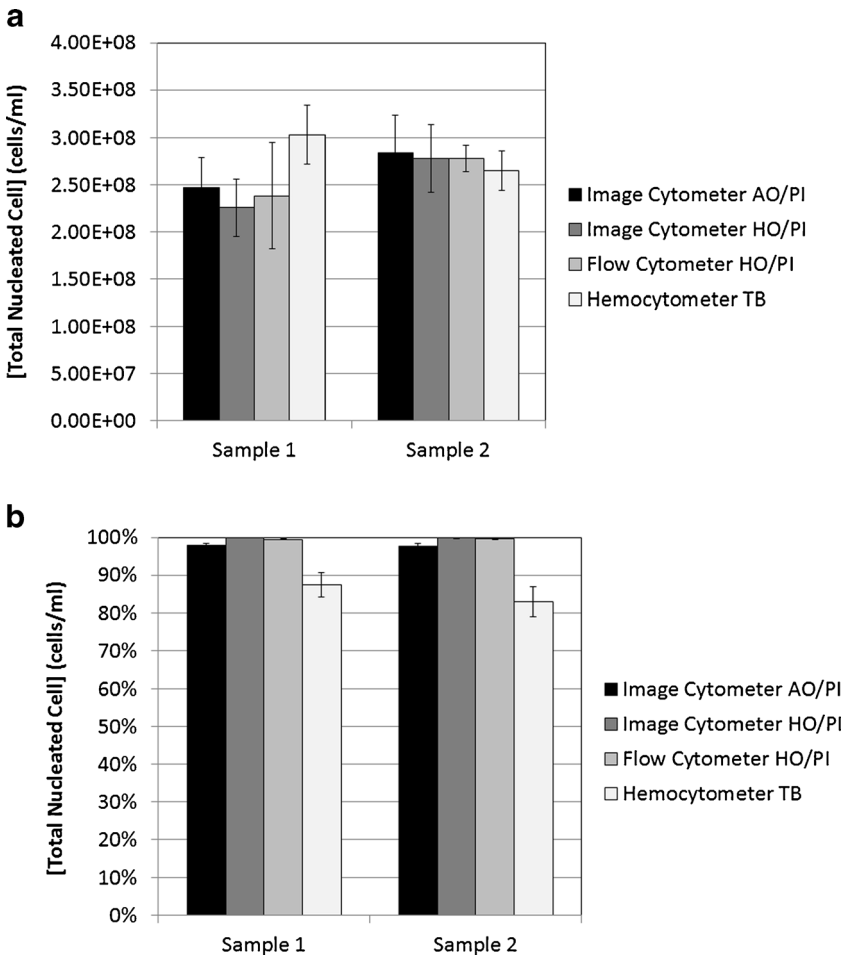

Fig. 4 Concentration and viability comparison results between hemocytometer, image and flow cytometry method. **a** Concentration and **b** viability bar graphs showing comparable measurements. For the sample 1 concentration measurement, the hemocytometer method showed approximately 10 % higher variation compared to image and flow cytometry. For viability measurements, both samples showed approximately ~15 % reduction in viability

count thousands of cells, which can improve the statistical analysis of the measurement. A 2-Sample *T* Test was conducted for comparing the detection methods for both samples.

Conclusion

In conclusion, the concentration and viability measurements using the three detection methods have shown comparable results. Viability results from the image cytometer using AO/PI and HO/PI were highly comparable to the flow cytometer data. Since fluorescent detection methods only stain nucleated cells, debris from adipose tissue does not interfere with viability and concentration counts, which can potentially provide more precise and consistent results in comparison to the manual hemocytometer method. The results have validated automated the image cytometry method for accurate SVF sample analysis, which can also improve the efficiency of SVF concentration and viability measurements. Although automated image-based AO/PI method has been shown previously, the previous publications have only discussed the possibility utilizing the staining method on various cell types. In this work, the automated methods can aid the research frontier in regenerative medicine by allowing researchers to quickly identify the quality of MSC samples in order to further their experimentations. Further study can be conducted to quantify the changes in SVF cell size or morphological information through automated image-based analysis [32].

Acknowledgments The authors would like to thank MediVet-America, Inc. (Nicholasville, KY) for their generous donation of the fresh canine adipose tissue samples.

Conflict of Interest The authors LLC, DK, BDP, and JQ declare a competing financial interest in that the work described in this manuscript used instrumentation and reagents provided by Nexcelom Bioscience LLC (Lawrence, MA). The performance of the instrumentation and reagents has been compared with standard approaches currently used in the biomedical industry.

References

1. Levi B, Longaker MT (2011) Adipose derived stromal cells for skeletal regenerative medicine. Stem Cells 29(4):576–582
2. Zuk PA (2010) The adipose-derived stem cell: looking back and looking ahead. Mol Biol Cell 21:1783–1787
3. Zuk PA et al (2002) Human adipose tissue is a source of multipotent stem cells. Mol Biol Cell 14:4279–4295
4. Jurgens WJFM et al (2008) Effect of tissue-harvesting site on yield of stem cells derived from adipose tissue: implications for cell-based therapies. Cell Tissue Res 332:415–426
5. Schäffler A, Büchler C (2007) Concise review: adipose tissue-derived stromal cells—basic and clinical implications for novel cell-based therapies. Stem Cells 25:818–827
6. Mohal JS, Tailor HD, Khan WS (2012) Sources of adult mesenchymal stem cells and their applicability for musculoskeletal applications. Curr Stem Cell Res Ther 7(2):103–109
7. Fan CG, Zhang QJ, Zhou JR (2011) Therapeutic potentials of mesenchymal stem cells derived from human umbilical cord. Stem Cell Rev 7(1):195–207
8. Huang YC et al (2009) Isolation of mesenchymal stem cells from human placental decidua basalis and resistance to hypoxia and serum deprivation. Stem Cell Rev 5(3):247–255
9. Fan J et al (2009) Synovium-derived mesenchymal stem cells: a new cell source for musculoskeletal regeneration. Tissue Eng Part B Rev 15(1):75–86
10. Nakao N et al (2010) Adipose tissue-derived mesenchymal stem cells facilitate hematopoiesis in vitro and in vivo: advantages over bone marrow-derived mesenchymal stem cells. Am J Pathol 177(2):547–554
11. Choudhery MS et al (2013) Comparison of human mesenchymal stem cells derived from adipose and cord tissue. Cytotherapy 15(3):330–343
12. Zuk PA et al (2001) Multilineage cells from human adipose tissue: implications for cell-based therapies. Tissue Eng 7(2):211–228
13. Mizuno H, Tobita M, Uysal AC (2012) Concise review: adipose-derived stem cells as a novel tool for future regenerative medicine. Stem Cells 30(5):804–810
14. Al Battah F et al (2011) Current status of human adipose-derived stem cells: differentiation into hepatocyte-like cells. Sci World J 11:1568–1581
15. Mazo M et al (2011) Adipose-derived stem cells for myocardial infarction. J Cardiovasc Transl Res 4(2):145–153
16. Lindroos B, Suuronen R, Miettinen S (2011) The potential of adipose stem cells in regenerative medicine. Stem Cell Rev 7(2):269–291
17. Zavan B et al (2010) Neural potential of adipose stem cells. Discov Med 10(50):37–43
18. Hong SJ, Traktuev DO, March KL (2010) Therapeutic potential of adipose-derived stem cells in vascular growth and tissue repair. Curr Opin Organ Transplant 15(1):86–91
19. Uysal AC, Mizuno H (2010) Tendon regeneration and repair with adipose derived stem cells. Curr Stem Cell Res Ther 5(2):161–167
20. Kim SC, Han DJ, Lee JY (2010) Adipose tissue derived stem cells for regeneration and differentiation into insulin-producing cells. Curr Stem Cell Res Ther 5(2):190–194
21. de Villiers JA, Houreld N, Abrahamse H (2009) Adipose derived stem cells and smooth muscle cells: implications for regenerative medicine. Stem Cell Rev 5(3):256–265
22. Rada T, Reis RL, Gomes ME (2009) Adipose tissue-derived stem cells and their application in bone and cartilage tissue engineering. Tissue Eng Part B Rev 15(2):113–125
23. Hoogendoorn RJ et al (2008) Adipose stem cells for intervertebral disc regeneration: current status and concepts for the future. J Cell Mol Med 12(6A):2205–2216
24. Riordan NH et al (2009) Non-expanded adipose stromal vascular fraction cell therapy for multiple sclerosis. J Transl Med 7:29
25. Astori G et al (2007) "In vitro" and multicolor phenotypic characterization of cell subpopulations identified in fresh human adipose tissue stromal vascular fraction and in the derived mesenchymal stem cells. J Transl Med 5:55
26. Chan LL et al (2012) Rapid image-based cytometry for comparison of fluorescent viability staining methods. J Fluoresc 22:1301–1311
27. Szabo SE et al (2004) Evaluation of an automated instrument for viability and concentration measurements of cryopreserved hematopoietic cells. Lab Hematol 10:109–111
28. Mascotti K, McCullough J, Burger SR (2000) HPC viability measurement: trypan blue versus acridine orange and propidium iodide. Transfusion 40:693–696

29. Foglieni C, Meoni C, Davalli AM (2001) Fluorescent dyes for cell viability: an application on prefixed conditions. Histochem Cell Biol 115:223–229
30. Jones KH, Senft JA (1985) An improved method to determine cell viability by simultaneous staining with fluorescein diacetate-propidium iodide. J Histochem Cytochem 33: 77–79
31. Tsaousis KT et al (2012) Time-dependent morphological alterations and viability of cultured human trabecular cells after exposure to Trypan blue. Clin Exp Ophthalmol 41(5):484–490
32. Surdo JL, Bauer SR (2012) Quantitative approaches to detect donor and passage differences in adipogenic potential and clonogenicity in human bone marrow-derived mesenchymal stem cells. Tissue Eng C Methods 18(11):877–889